

A Comparison of Change Detection Methods Using Multispectral Scanner Data

By Paul M. Seevers, Brenda K. Jones, Zhicheng Qiu, and Yutong Liu



▲ Dallas-Ft. Worth Area
March 12, 1974

▼ Dallas-Ft. Worth Area
March 22, 1989



A Comparison of Change Detection Methods Using Multispectral Scanner Data

By Paul M. Seevers, Brenda K. Jones, Zhicheng Qiu, and Yutong Liu

Open-File Report No. 93-355

UNITED STATES
DEPARTMENT OF THE INTERIOR
U.S. GEOLOGICAL SURVEY

TABLE OF CONTENTS

ABSTRACT	1
INTRODUCTION	2
METHODS.....	3
Data Selection	3
Data Processing	3
Change Detection Methods Evaluated.....	4
RESULTS AND DISCUSSION	6
CONCLUSIONS	14
REFERENCES	15
APPENDIX	16
Fast Classification Method	16

A COMPARISON OF CHANGE DETECTION METHODS USING MULTISPECTRAL SCANNER DATA

By Paul M. Seevers¹, Brenda K. Jones¹, Zhicheng Qiu², and Yutong Liu²

ABSTRACT

Change detection methods were investigated as a cooperative activity between the U.S. Geological Survey and the National Bureau of Surveying and Mapping, People's Republic of China. Subtraction of band 2, band 3, normalized difference vegetation index, and tasseled cap bands 1 and 2 data from two multispectral scanner images were tested using two sites in the United States and one in the People's Republic of China. A new statistical method also was tested. Band 2 subtraction gives the best results for detecting change from vegetative cover to urban development. The statistical method identifies areas that have changed and uses a fast classification algorithm to classify the original data of the changed areas by land cover type present for each image date.

¹ Hughes STX Corporation. Work performed under U.S. Geological Survey contract 1434-92-C-40004.

² Research Institute of Surveying and Mapping, National Bureau of Surveying and Mapping, People's Republic of China.

Any use of trade, product, or firm names is for descriptive purposes only and does not imply endorsement by the U.S. Government.

INTRODUCTION

An investigation of change detection methods was undertaken in 1992 as one of several cooperative activities between the EROS Data Center, U.S. Geological Survey, and the National Bureau of Surveying and Mapping (NBSM), People's Republic of China. This activity was a part of a formal Protocol in Surveying and Mapping between the United States and the People's Republic of China.

A review of the literature regarding methods of change detection showed a variety of approaches. Singh (1989) suggests that the approaches can be categorized as two types: (1) comparative analysis of data of different dates and (2) simultaneous analysis of multitemporal data. He lists the methods as differencing (including vegetation index differencing), ratioing, regression, principal components, change vector, and postclassification comparison.

Of the above methods, differencing is the most widely used. The simplest form of differencing is the subtraction of the values of a single band of data taken on two different dates. Singh (1989) describes a variety of research efforts related to this method showing varied success. Much of this effort dealt with the establishment of threshold boundaries between change and no-change pixels in the histogram of a difference image. It is assumed that the ground area sampled by the same image pixel location on two different dates will not coincide. Hence, the number of subtraction values equal to zero will be very small, even if no significant ground cover changes have occurred. The difficulty the analyst faces is to define what level of pixel value difference defines the changes that are being assessed.

A second method appearing frequently in the cited literature is principal components analysis. Change detection using this method can be assessed from two 4-band images as image differencing or regression analysis of the principal components bands or as principal components of an 8-band image. The major component images of the latter procedure show major differences and the minor component images minor changes (Byrne and others, 1980).

The remaining methods are used less frequently. Regardless of the method used, the results are rarely satisfactory to the investigators. Two methods applied to the same site always give different results. The cited literature shows that some methods are better for certain kinds of change detection than others, suggesting a strong dependency on scene content.

This study was designed to compare selected change detection methods, using scenes with different land cover characteristics and different types of land cover change. The same differencing procedure was used for each image pair to show the advantages and disadvantages of each method based on the land cover characteristics and changes to be defined in each image pair. A new statistical method created by NBSM personnel was also evaluated.

METHODS

Data Selection

Multispectral scanner data have been collected since the launch of the first Landsat in 1972, providing a broad selection of change pairs for testing change detection methods. Site selections were made to maximize the time difference between image dates, which were cloud free, and provide different land cover types in which to detect and assess change.

The selected images were of the Dallas-Ft. Worth, Texas, Mount St. Helens, Washington, and the Shanghai area in the People's Republic of China. Image dates for the Dallas-Ft. Worth area were March 12, 1974, and March 22, 1989. Because of the population growth of this metropolitan area there was significant conversion of agricultural land to urban housing. The agricultural land was a combination of cropland and grassland, providing a mixed pattern of land use.

The Mount St. Helens image dates were September 15, 1973, and August 31, 1988. Eruption of this volcano in 1980 resulted in considerable ash deposit and vegetation damage in the vicinity of the summit. In addition, logging activity had created numerous areas where timber had been completely removed, and the clearcut areas were in various stages of regrowth. Remaining vegetation ranged from dense stands of coniferous forest to shrub grasslands in the drier, flatter areas.

Image dates for the Shanghai area were May 11, 1978, and May 13, 1991. The population growth within this intensive agricultural area resulted in expansion of the urban area of Shanghai, as well as the areas of many of the villages scattered throughout the cropland. Silt deposits in the delta of the Yangtze River also changed the shapes of islands. There were clouds present in the 1991 image, which added an undesirable component to the change detection process.

In each case, the images selected were as close as possible relative to day within the year. This minimized any seasonal change in vegetation. If there were climatic differences, such as precipitation amount, between the image dates, they could conceivably create detectable differences by the methods being evaluated.

Data Processing

The images for the Dallas-Ft. Worth and Mount St. Helens areas were registered to a map base in the universal transverse mercator projection and resampled to 50-m cells using the cubic convolution algorithm. Data for the Shanghai area were registered image-to-image because of a lack of appropriate maps for map base registration. They were also resampled to 50-m pixels using the cubic convolution algorithm. A second evaluation of the Shanghai data, conducted by NBSM personnel after the initial comparisons, used data registered to a map base and resampled to 60-m cells using the nearest neighbor algorithm.

A subset of each image pair, focused on the area of interest, was extracted. These subsets were calibrated to radiance values using coefficients published by Price (1987). Normalized difference vegetation index (NDVI) images of the calibrated subsets were also created using the following calculation:

$$NDVI = \left[\frac{\text{Infrared band (3)} - \text{red band (2)}}{\text{Infrared band (3)} + \text{red band (2)}} + 1 \right] * 100$$

The four bands of each calibrated subset were used in the Land Analysis System algorithm TASSELCP to create the tasseled cap transformations of each image. This algorithm uses predefined coefficients for the bands created, as contrasted with a principal components analysis, which uses statistical data to define the coefficients.

Change Detection Methods Evaluated

Five differencing methods and a statistical method created by NBSM personnel were evaluated. The five differencing methods were: (1) subtraction of band 2, (2) subtraction of band 3, (3) subtraction of NDVI band, (4) subtraction of tasseled cap band 1, and (5) subtraction of tasseled cap band 2. Where the subtraction procedure was used, the older date of the image pair was subtracted from the more recent date. These subtractions produced a range of values, both positive and negative, with a maximum number of values near zero. Each result was mapped to values from zero to 255 to create positive values that could be displayed on the image processing system. Based on past experience and visual examination of the image values, it was determined that values within ± 1.5 standard deviations of the mode of the data represented insignificant change. Values beyond ± 1.5 standard deviations represented significant change, positive values meaning an increase in the spectral values and negative values meaning a decrease in the spectral values for the more recent image. Gain or loss of spectral intensity can be associated with different kinds of landscape changes.

The statistical method developed by NBSM personnel required the selection of training areas in land cover types common to and unchanged within both images of a change pair. Because this was the first use of this method, training areas were taken only for water, predominant vegetation, and nonvegetated (urban or ash covered) land cover. A minimum of three training areas for each land cover type for each image was selected. The training areas for each land cover type were combined and a mean and standard deviation calculated for each of the cover types. A change value was calculated for each cover type using the following equation:

$$CH_K = \frac{1}{n} \sum_{i=1}^n \left| MG_{t1,i}^K - MG_{t2,i}^K \right| \frac{2}{n} \sum_{i=1}^n \left| SD_{t1,i}^K - SD_{t2,i}^K \right| \quad (1)$$

where

- CH = change value
- K = land cover number
- n = number of bands
- t1 = older image
- t2 = more recent image
- i = band number
- MG = mean value
- SD = standard deviation

These change values were used to define an upper and lower change threshold for each of the cover types. The calculations were:

$$TH_{K1} = \alpha_K CH_K \quad (2)$$

$$TH_{K2} = \beta_K CH_K \quad (3)$$

where

- TH_{K1} = threshold to define no-change area for K
- K = land cover number
- TH_{K2} = threshold to define change area for K
- α_K = no-change factor
- β_K = change factor

The change and no-change factors set a range of mean values for each cover type from which to determine if change has occurred. This range is somewhat analogous to the bounds placed on the standard deviation range defined in the differencing method. The analyst must define the two factors by evaluating the change areas resulting from the application of the factors to the image. Depending on the alteration required to better define the change, the factors can be adjusted to vary the area defined as changed. Two or three iterations of factor value changes were usually sufficient to determine which values best defined change areas.

The next step was to define change areas within the image pair. Using the most recent image, an 8- by 8-pixel window was used to grid the image and to calculate a mean for each window for each band. These mean values were classified by cover type using a minimum distance algorithm and the statistics from the training areas. Equation 1 was used to calculate a change value, using the window cover type, mean, and standard deviation. The resulting change value was compared with the change threshold values previously defined. If the change value was smaller than TH_{K1} , the window had no change. If the change value was larger than TH_{K2} , the window had change. If the value was between TH_{K1} and TH_{K2} the window was subdivided into four 4- by 4-pixel windows and new change values were computed for the subdivisions (equation 1). A second threshold was calculated for the window subdivisions:

$$TH_K = (TH_{K1} + TH_{K2})/2 \quad (4)$$

where TH_K = second change threshold
 TH_{K1} = no-change threshold from previous calculation
 TH_{K2} = change threshold from previous calculation

If the change value of the window subdivision was smaller than TH_K , there was no change. If the change value was larger than TH_K , it represented an area of change.

When the areas of change were identified, a classification was performed on the change areas to identify the cover type for those areas in each image. The statistics from the original training areas were used in a newly devised fast classification algorithm. This algorithm uses a parallelepiped classifier in combination with a simplified approach to a probability density function decision process. When the parallelepiped classifier was unable to resolve in which class a pixel belonged, the pixel was entered into the simplified probability density function process. This process approximates the overlap point between the density curves using straight lines based on the distribution mean, maximum, minimum, and standard deviation for the two types being considered. A minimum distance rule was applied to a pixel value and assigned to a cover type based on its weighted distance from the type means. This classification was carried out on both dates of the image pairs. See the appendix for a detailed explanation of the process.

After classification of the change areas of both images, a contingency table was created to determine if the same cover type existed in the change areas for both images. If change had occurred between the two image dates, the pixels that were a specific cover class on one date would not be that same cover class on the second date. Those pixels that were the same cover class for both dates were redefined as no-change pixels. Percent of cover class change was calculated for each cover class for each image date.

RESULTS AND DISCUSSION

To evaluate each method, an image was produced that contained areas identified as change or no change for each of the three sites. To facilitate the further manipulation of the data, each difference image was processed with a nominal filtering procedure to eliminate homogeneous areas less than 9 acres in size. Nominal filtering (Fosnight, 1987) systematically reassigned pixel values of designated homogeneous area polygons to values of the surrounding areas. The resulting raster images were converted to polygons by importing them into Arc/Info. In Arc/Info the polygon boundaries were converted to lines and the lines were converted to a raster image. For each change detection method, the raster polygon boundaries were imbedded in a color-infrared composite of the most recent date of each change pair. Polygons surrounded by a white border (figs. 3-7) were those areas identified as changed.

The Dallas-Ft. Worth change pair provides an example of results achieved by each method. Land cover for the two dates is shown by figures 1 and 2. Figures 3-7 show results of the subtraction of band 2, band 3, NDVI, tasseled cap band 1, and tasseled cap band 2 data from the two images. Change from agricultural to urban land use was the primary focus for this change pair. Comparison among the methods shows the variable results obtained for identification of this change. In addition, varying numbers of polygons show changes within the agricultural and urban areas.



Figure 1. Multispectral scanner false-color composite of the Dallas-Ft. Worth area. Data acquired March 22, 1989.



Figure 2. Multispectral scanner false-color composite of the Dallas-Ft. Worth area. Data acquired March 12, 1974.



Figure 3. March 22, 1989, composite of Dallas-Ft. Worth area showing polygons enclosed by white lines that were identified as change areas by subtraction of band 2 for the 1974 and 1989 images.



Figure 4. March 22, 1989, composite of Dallas-Ft. Worth area showing polygons enclosed by white lines that were identified as change areas by subtraction of band 3 for the 1974 and 1989 images.

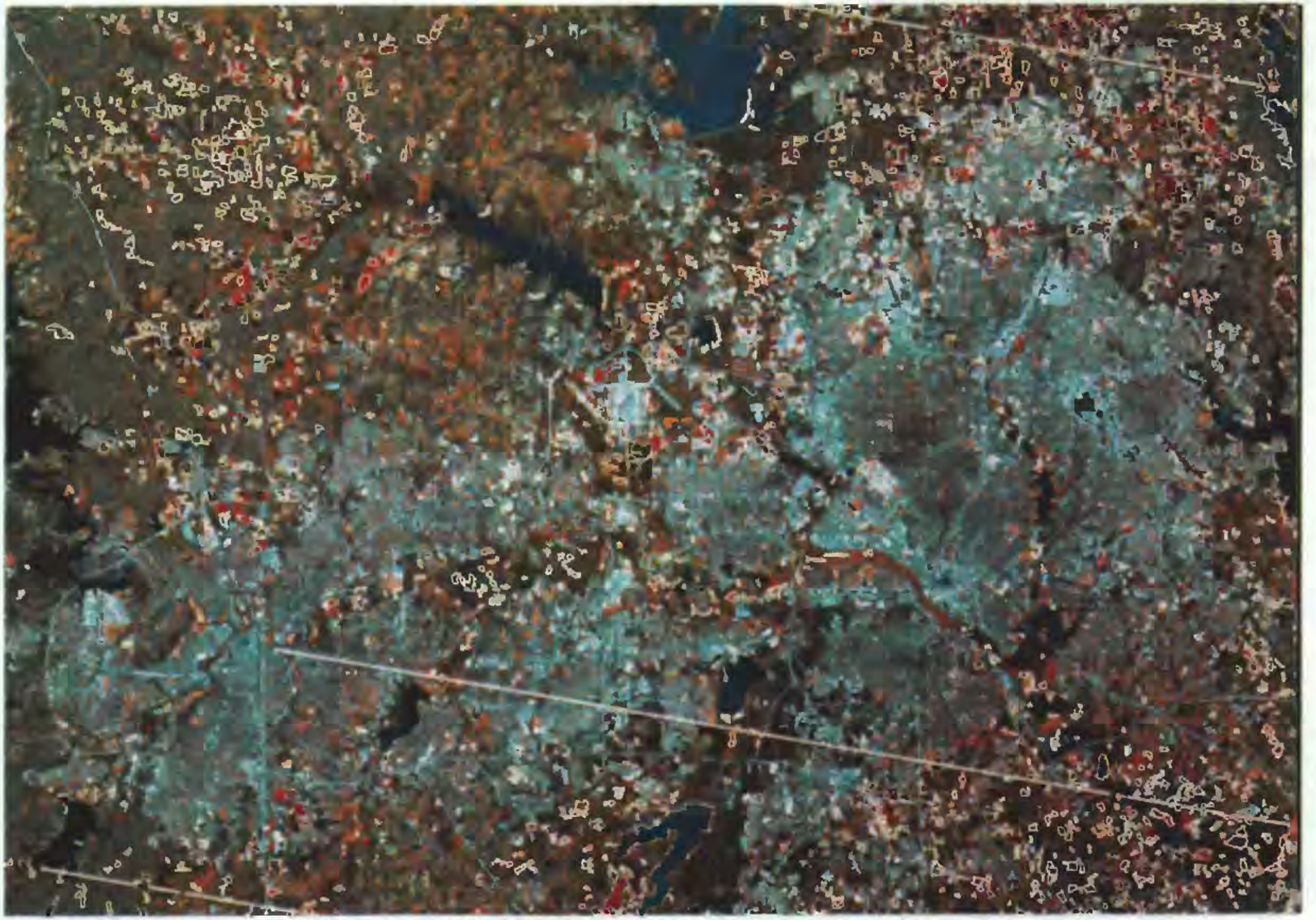


Figure 5. March 22, 1989, composite of Dallas-Ft. Worth area showing polygons enclosed by white lines that were identified as change areas by subtraction of normalized difference vegetation index images produced from the 1974 and 1989 images.



Figure 6. March 22, 1989, composite of Dallas-Ft. Worth area showing polygons enclosed by white lines that were identified as change areas by subtraction of tasseled cap band 1 images.



Figure 7. March 22, 1989, composite of Dallas-Ft. Worth area showing polygons enclosed by white lines that were identified as change areas by subtraction of tasseled cap band 2 images produced from the 1974 and 1989 images.

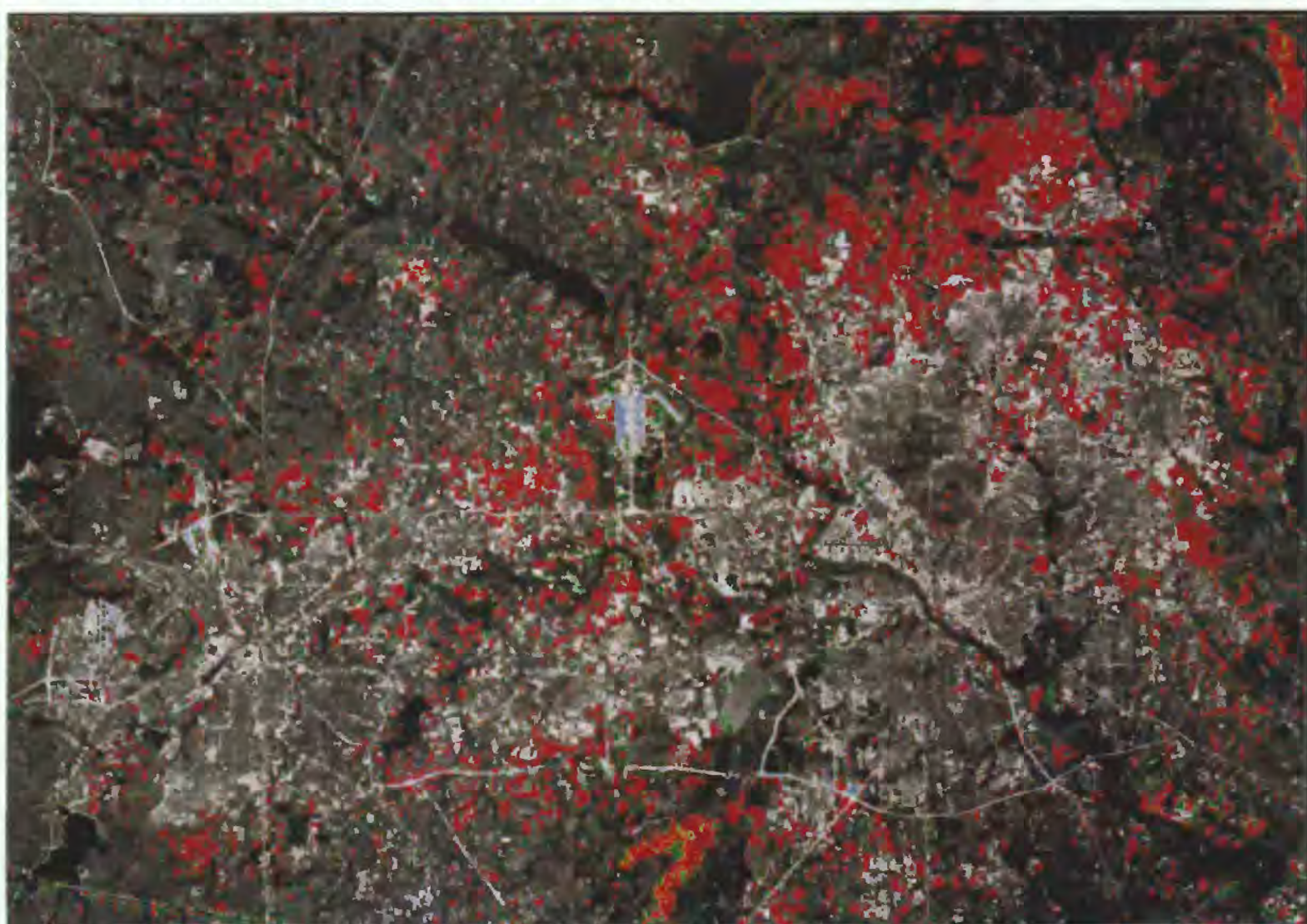


Figure 8. Colors show areas identified as changed using the statistical method and classified by cover type on the 1974 image. Red represents vegetation, green represents urban, and blue represents water. Background image is the visible red band of the 1974 image.

The results of the NBSM method were shown as images identifying the types of land cover that had been classified as changed. Figures 8 and 9 show the results of the NBSM method for the Dallas-Ft. Worth change pair. Within the changed areas, each cover type was given a unique color to visually assess the correctness of the change determination. Because a classification of change areas was performed on each image, the change areas were the same on each image and the cover types indicated the change that had occurred.

The second evaluation of the Shanghai image pair by NBSM personnel demonstrated the use of the statistical method to identify changed pixels and classify them by land cover. Table 1 shows what changes occurred within 21 districts and counties in Shanghai and the surrounding area. Ground data were not available to determine the accuracy of these changes.

District or County	Land cover classes ¹						Total area changed	Total area in district or county
	1978			1991				
	water	urban	veg.	water	urban	veg.		
1	0	0	3.93	0	3.93	0	3.93	22.29
2	0	0.01	6.43	0	6.43	0.01	6.44	28.83
3	0	0.02	7.76	0	7.76	0.02	7.78	51.43
4	0	0.08	18.35	0	18.35	0.08	18.43	253.29
5	1.08	9.72	22.68	0	23.32	10.16	33.48	1274.01
6	0	0	5.96	0	5.96	0	5.96	30.52
7	0	0	0	0	0	0	0	6.92
8	0	0	1.44	0	1.44	0	1.44	18.12
9	0	0.05	4.42	0	4.42	0.05	4.47	25.16
10	0	0.03	9.35	0	9.35	0.03	9.38	43.45
11	0	0	0	0	0	0	0	8.82
12	0	0	3.80	0	3.80	0	3.80	20.84
13	0	0.07	13.57	0	13.57	0.07	13.64	301.71
14	0	0	3.69	0	3.69	0	3.69	251.69
15	0	0.02	10.89	0	10.89	0.02	10.91	451.41
16	0	0.07	15.63	0	15.63	0.07	15.70	481.76
17	0	0.28	10.86	0	10.86	0.28	11.14	448.65
18	0	0	0.93	0	0.93	0	0.93	11.52
19	0	0.03	3.09	0	3.09	0.03	3.12	292.95
20	0	0.11	21.21	0	21.21	0.11	21.32	63.28
21	0.14	0.36	1.95	0	2.03	0.42	2.45	141.99

Table 1. Results of statistical method showing the land cover changes that were identified on the Shanghai change pair image in square kilometers.

¹ This number is the area defined as changed and classified as that land cover type for the indicated image date.



Figure 9. Colors show areas identified as changed using the statistical method and classified by cover type on the 1989 image. Red represents vegetation, green represents urban, and blue represents water. Background image is the visible red band of the 1989 image.

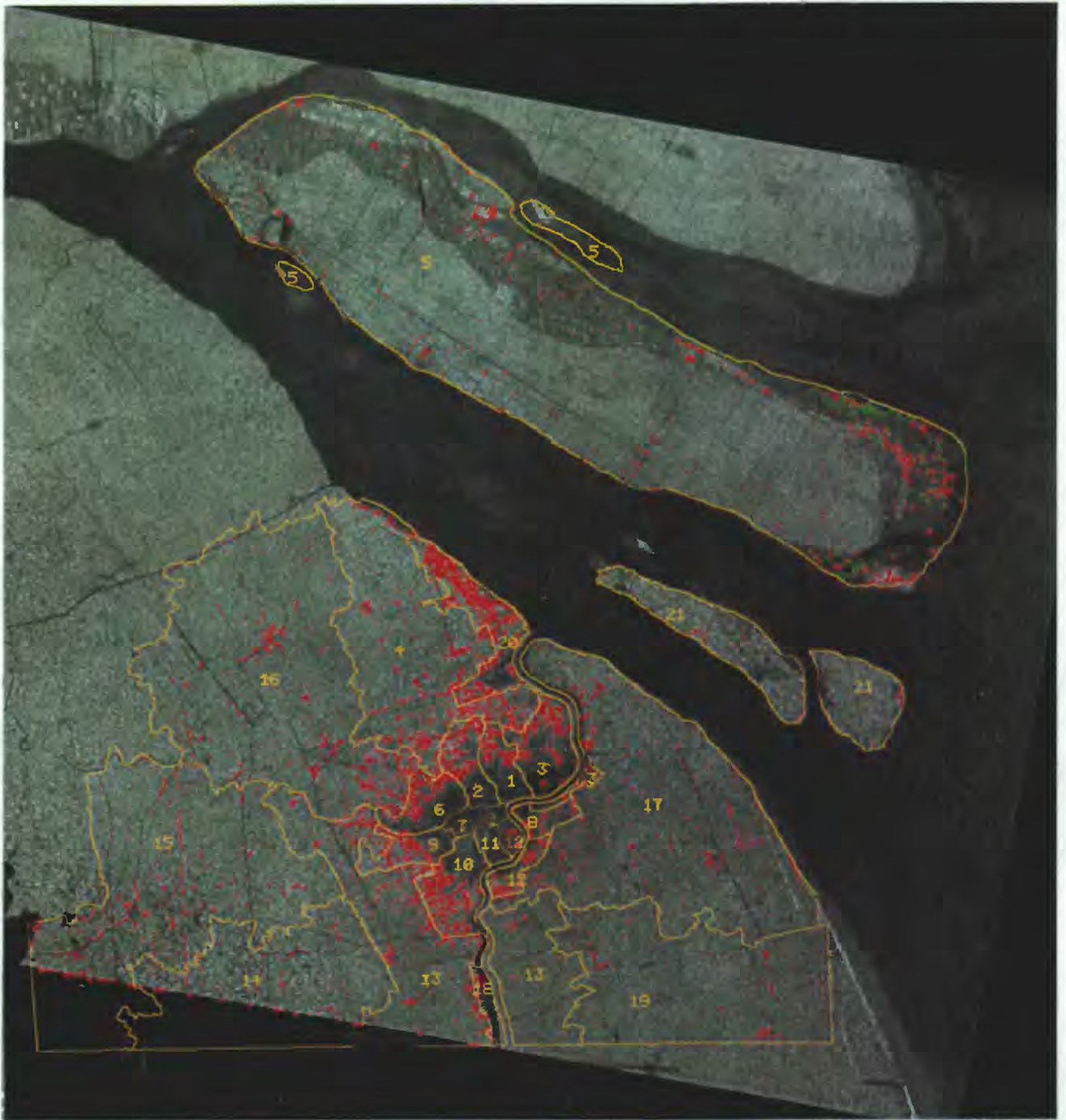


Figure 10. Numbers identify districts or counties in and around Shanghai, People's Republic of China, where changes were detected using the statistical method. Classification of the change areas in the 1978 image identifies red areas as vegetation and green areas as urban. Background image is near-infrared band of 1978 image.

Figure 10 shows the district or county boundaries associated with the region and the areas identified as changed within each bounded area.

Quantitative assessment of the accuracy of the change detection methods was not possible because of the lack of ground data. However, visual comparisons were made between the imbedded polygon images and the earlier date for each change pair as to the correctness of change areas defined by the polygon boundaries. Because of the high number of change polygons it was only possible to gain a general

impression of how well the change areas were defined. Based on this observation, the results suggest that the band 2 subtraction method best depicted the urban development in the Dallas-Ft. Worth area. Urban development in Shanghai and surrounding villages was best shown by the NDVI subtraction method. Changes caused by the eruption of Mount St. Helens were shown best by the band 2 subtraction method.

None of the methods produced an optimum identification of major changes within an image pair. As indicated earlier, simple subtraction of pixel values resulted in some value near zero for almost every pixel location in an image pair. This required further manipulation of the difference data to identify what the analyst wanted to depict as changed. In this study the further manipulation was the imposition of a threshold on the magnitude of difference. A threshold sets the boundaries of the change and no-change difference values and shows that if significant changes in land cover have occurred, a significant change in spectral reflectance would also occur. The analyst must decide what constitutes a significant level of change. This assumes that the portion of the electromagnetic spectrum from which the data were collected shows the reflectance change. The imposition of a threshold is a nonspecific means of selecting change values as they relate to land cover types. This results in a variety of land cover types being identified as changed.

The fact that there is a value near zero for nearly every pixel location is influenced by a number of factors, such as image registration, data calibration, atmospheric interference, illumination conditions, climatic variation, and differing instantaneous fields of view (IFOV). It is not clear what effect each of these factors has on the pixel radiance values. It would seem that differing IFOV's have a high probability of being a major factor. Given the spectral variability that exists within land cover, the expectation is that each pixel is sampling a slightly different portion of the landscape than its change pair counterpart and providing a slightly different reflectance value. The object of the statistical method was to define land cover in the context of the existing variability and to define change as radiance differences beyond the expected variability. As with any supervised classification, the uncertainty is whether the land cover type variability is adequately defined. However, the approach does allow the analyst to focus on the land cover types whose changes are being considered. Also, it allows the analyst to identify land cover types that are being changed and to what types they are being changed.

CONCLUSIONS

Of the six methods of change detection evaluated, the subtraction of band 2 is more applicable, when considering change from vegetated to nonvegetated areas. The tasseled cap bands 1 and 2 are the least discriminatory of the methods. All methods suffer from the inability to limit the discrimination to a specific type of cover change. The NBSM method can separate changes into cover types, but has commission and omission errors relative to each cover type. These results suggest that the land cover characteristics of the scene and the type of change to be determined will indicate what method of change detection will be most successful.

REFERENCES

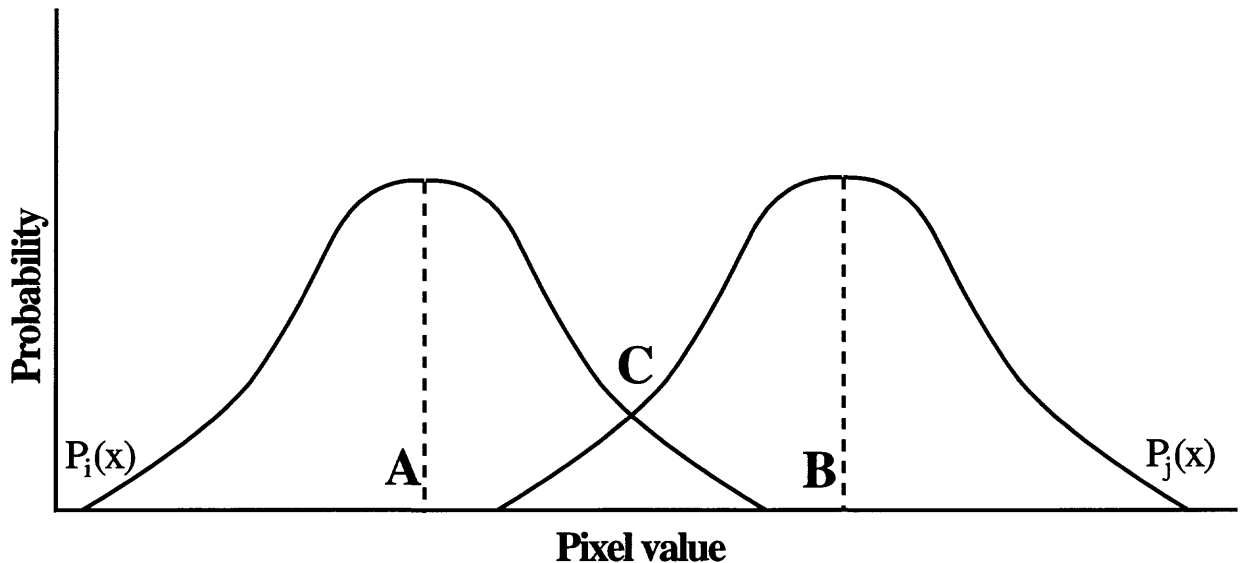
- Byrne, G.F., Crapper, P.F., and Mayo, K.K., 1980, Monitoring land cover change by principal component analysis of multitemporal Landsat data: *Remote Sensing of Environment*, v. 10, p. 175-184.
- Fosnight, E.A., 1987, Applications of spatial postclassification models: *International Symposium on Remote Sensing of Environment*, Ann Arbor, Michigan, October 26-30, 1987, Proceedings, p. 469-485.
- Price, J.C., 1987, Calibration of satellite radiometers and the comparison of vegetation indices: *Remote Sensing of Environment*, v. 21, p. 15-27.
- Singh, A., 1989, Digital change detection techniques using remotely sensed data: *International Journal of Remote Sensing*, v. 10, no. 6, p. 989-1003.

APPENDIX

Fast Classification Method

Data to be classified are entered into a parallelepiped classifier, which uses the mean and standard deviation of the training areas to define rectangular decision regions. Not all pixels fall within these regions. In these cases the pixels are submitted to a modified maximum likelihood decision rule classifier.

This modified decision rule classifier is based on the assumption of normal distribution for spectral response. Given a mean and standard deviation, a probability density function can be calculated to define the statistical probability of a pixel value being a member of a particular land cover type. For a one-dimensional probability density function involving two land cover types the boundaries can be defined by $P_i(x)$ and $P_j(x)$, shown by figure 11.



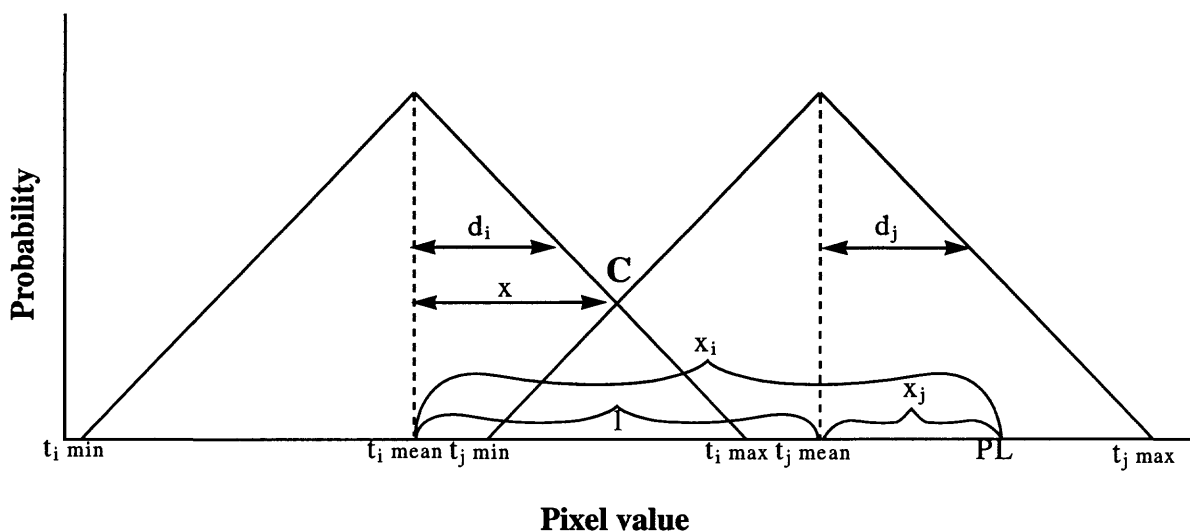
A = mean value of land cover type *i*

B = mean value of land cover type *j*

C = crossover point of probability density function curves $P_i(x)$ and $P_j(x)$

Figure 11. Probability density function curves showing boundaries defined by two land cover types.

Typical maximum likelihood classification requires that the probability of the pixel value occurring in each available land cover type be calculated and then assigned to the land cover type where the probability values fit the best. To avoid the large number of probability calculations, the procedure was modified. The intersection point of the probability density function curves were used to distinguish between the two land cover types. To define the probability density function curves, the minimum, maximum, mean, and standard deviation were used. Rather than calculating a normal distribution curve, distribution relationships were established using straight lines (fig. 12).



- c = crossover point between probability density functions for type i and type j
- d_i = standard deviation of type i
- d_j = standard deviation of type j
- PL = pixel location of pixel being classified
- l = units between type means
- x = units between type i mean and crossover point
- x_i = units between type i mean and pixel location
- x_j = units between type j mean and pixel location
- $t_i \text{ min}$ = minimum value for type i
- $t_i \text{ max}$ = maximum value for type i
- $t_j \text{ min}$ = minimum value for type j
- $t_j \text{ max}$ = maximum value for type j
- $t_i \text{ mean}$ = mean value for type i
- $t_j \text{ mean}$ = mean value for type j

Figure 12. Distribution relationships established using straight lines rather than probability density function curves.

The relationship between the crossover point and the standard deviations is shown in figure 12. The position of point C can be calculated:

$$x = \frac{d_i}{d_i + d_j} \cdot 1$$

Weighting factors are calculated next:

$$w_i = \frac{x}{1} = \frac{d_i}{d_i + d_j}$$

$$w_j = \frac{1-x}{1} = \frac{d_j}{d_i + d_j}$$

where w_i = weighting factor for type i

w_j = weighting factor for type j

The modified distances between PL and type i and type j means are calculated:

$$S_i = w_j \cdot x_i$$

$$S_j = w_i \cdot x_j$$

where S_i = modified distance between PL (fig. 12) and type i mean

S_j = modified distance between PL (fig. 12) and type j mean

Pixel PL is assigned to a type based on the minimum distance to a mean.

For classification of multiband images, S_i and S_j can be calculated by the following formulas:

$$S_i = \sum_{a=1}^{nc} (x_i - \mu_{ia}) w_{ja}$$

$$S_j = \sum_{a=1}^{nc} (x_j - \mu_{ja}) w_{ia}$$

where: nc = number of bands

a = band number

x_i = units between type i mean and pixel location (fig. 2)

μ_{ia} = mean value of band a for type i

μ_{ja} = mean value of band a for type j

w_{ia} = weighting coefficient for band a, type i

w_{ja} = weighting coefficient for band a, type j